

Time Resolved Studies of Proton Irradiated Quantum Dots

Saulius Marcinkevičius

Department of Microelectronics and Information Technology, Royal Institute of Technology, Electrum 229, 16440 Kista, Sweden

Rosa Leon

Jet Propulsion Laboratory, California Institute of Technology, 4800 Oak Grove Drive, Pasadena, CA 91109, U.S.A.

Charlene Lobo

Cavendish Laboratory, University of Cambridge, Madingley Road, Cambridge CB3 0HE, U.K.

Brian Magness and William Taylor

Department of Physics and Astronomy, California State University, Los Angeles, CA 90032, U.S.A.

ABSTRACT

The effects of proton irradiation on carrier dynamics were measured by time-resolved photoluminescence on InGaAs/GaAs quantum dot structures with different dot density and substrate orientation, as well as on InAlAs/AlGaAs quantum dots. Results were compared to irradiation effects on carrier dynamics in thin InGaAs quantum wells. We find that carrier lifetimes in QDs are much less affected by proton irradiation than in quantum wells, which can be attributed to the three-dimensional carrier confinement in quantum dots.

INTRODUCTION

Proton irradiation can induce structural defects and creates carrier-trapping centers in semiconductors. These defects have been used to an advantage when fabricating semi-insulating layers and ultrafast microwave devices. However, since protons have sufficient mass to cause displacement damage, their effects may be detrimental to the device performance when nonradiative carrier recombination is not desired, as is the case in most optoelectronic device applications.

Studies of steady-state optical properties in proton-irradiated quantum dot (QD) structures [1] and in proton-irradiated QD lasers [2] showed that the QDs structures and QD based devices are much more resistant to irradiation than bulk semiconductors or quantum wells (QW). These studies showed not only better radiation tolerance, but also an increase in either photoluminescence (PL) intensities [1] or laser performance [3] with low proton or ion fluences. In the present work we have extended these investigations by studying carrier dynamics in irradiated QD structures. In order to obtain a better understanding of the effects of proton induced displacement damage on QD carrier dynamics, several types of structures were investigated: different materials compositions, surface QD densities, and substrate orientations.

EXPERIMENTAL DETAILS

InGaAs/GaAs (100), InAlAs/AlGaAs (100) and InGaAs/GaAs (311)B QDs were grown by metal-organic chemical-vapor deposition in a horizontal reactor cell operating at 76 Torr. Trimethylgallium, trimethylindium, trimethylaluminum (for growth of InAlAs and AlGaAs) and

Table I. Data summary for investigated QD and QW structures.

Structure and material dot/barrier	Surface density (in dots/cm ²)	Average diameter (nm)	Average aspect ratio (height/diameter)	80 K PL peak energy (eV)
InGaAs/GaAs quantum well	—————	1 nm width	—————	1.35
Low density InGaAs/GaAs (100) QDs	4×10^8	25 ± 5	1/6	1.06 (ground state)
High density InGaAs/GaAs (100) QDs	2×10^{10}	25 ± 5	1/6	1.18
InGaAs/GaAs (311)B QDs	3×10^{10}	25 ± 5	1/8	1.32
InAlAs/AlGaAs (100) QDs	1×10^{11}	20 ± 5	1/6	1.82

arsine were used as precursors. For the InGaAs QDs, growth of a 50 nm GaAs buffer layer at 650 °C was followed by deposition of 1.5 nm InGaAs with a nominal indium mole fraction of 0.6. Different surface densities of InGaAs QDs in similar sizes were obtained by changing the arsine partial pressures during growth of the QDs [4]. InGaAs quantum wells (QW) were obtained by stopping the growth of InGaAs before the onset of the Stranski-Krastanow transformation, giving thin (1 nm) QWs. For the InAlAs/AlGaAs QDs, growth of a 500 nm AlGaAs buffer layer at 775 °C and nominal aluminum mole fraction of 0.35 was followed by deposition of 1.5 nm InAlAs with nominal indium mole fraction of 0.55. The QDs were then capped with 100 nm GaAs (AlGaAs) layers, deposited while the temperature was gradually raised to 600 (700) °C. When AlGaAs barriers were used, a final 10 nm GaAs capping layer was deposited to prevent surface oxidation. Atomic force microscopy and transmission electron microscopy were used to give information on island sizes and surface densities in capped and uncapped InGaAs and InAlAs QDs. Proton irradiation was carried out using a Van De Graaff accelerator. Samples were irradiated at room temperature using 1.5 MeV protons at five different doses ranging from 1.3×10^{11} to 3.5×10^{13} cm⁻², with a dose rate of $\sim 6 \times 10^{12}$ protons/sec. Dose uniformity was monitored using radiochromic film at low doses.

Table I presents a summary of the different structures used in this study, showing their materials and structural properties (dot sizes, aspect ratios and concentrations) as well as the energy of their PL intensity maximum. It is worth noting that the InGaAs/GaAs (311)B QDs have similar diameters, but form in slightly higher surface concentrations and have a smaller aspect ratio than InGaAs/GaAs (100) QDs. Since the dimensions in the growth direction dominate quantum confinement energies, their corresponding PL emission peaks are at higher energies [5]. High density InGaAs QDs exhibit a blue shift of the PL emission energy with respect to the low density InGaAs QDs. These differences are not seen to correspond to variations in dot sizes or compositions, but rather have been ascribed to progressive strain

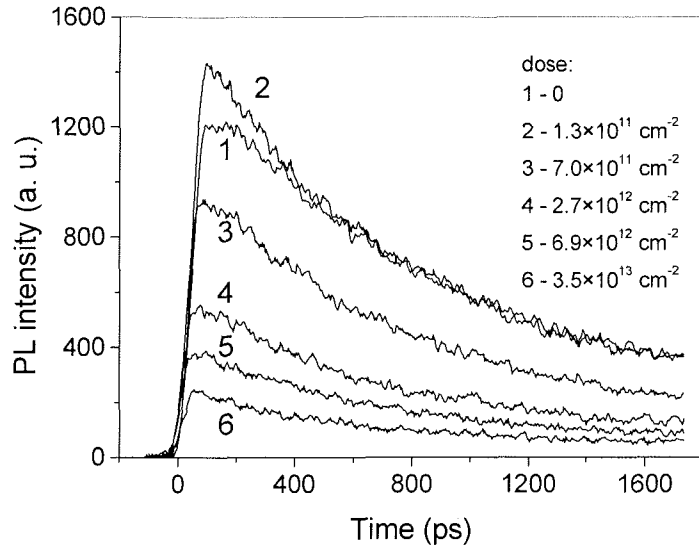


Figure 1. PL intensity vs. time for high surface density InGaAs QDs for different proton doses.

RESULTS AND DISCUSSION

Time-resolved PL was measured on all structures described in Table I. Figure 1 shows PL transients for the high surface density InGaAs/GaAs (100) QD samples irradiated with different proton doses. The variation of PL peak intensities and decay times shown in Figures 2 and 3 are extracted from Figure 1 and single exponential fits of PL decay curves. Figure 2 shows the observed changes in PL intensity as a function of proton dose for all samples. Figure 3 shows the variation in PL decay times.

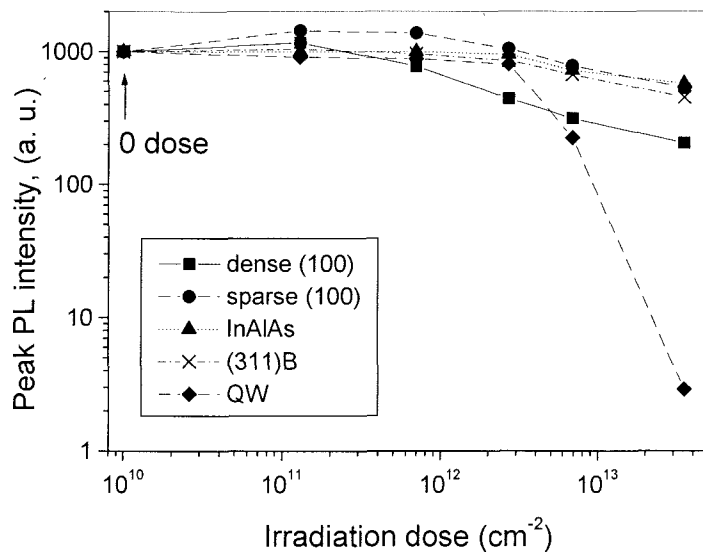


Figure 2. Changes in PL peak intensities for different QD structures and QW as a function of proton fluence.

deformation of the QD confining potentials, which result in shallower effective confinement as the dot density increases [6].

Carrier dynamics were studied by time-resolved photoluminescence (PL) at 80 K after excitation by a short laser pulse from a self mode-locking Ti:sapphire laser (pulse duration 80 fs, repetition frequency 95 MHz). The excitation wavelength was 800 nm for the InGaAs structures and 400 nm for the InAlAs QDs. For the PL detection, either an upconversion set-up with a temporal resolution of 150 fs or a synchroscan streak camera (resolution 3 ps) were used.

As can be seen in Figure 3, the carrier lifetimes in QDs are much less affected by proton irradiation than in the QWs or the wetting layer (WL) in the QD structures. For example, the 80 K carrier lifetimes in (311)B QDs decrease from 2.2 ns for the unirradiated sample to 1.4 ns for the sample with the highest proton dose, compared to a ~20-fold and ~40-fold decrease for the QW and the WL, respectively. Similar trends are observed for all QD samples. Moreover, similarly as in the steady-state PL measurements [1], we observe an increase in the QD PL intensity (most prominent in the low-density InGaAs (100) QDs) with

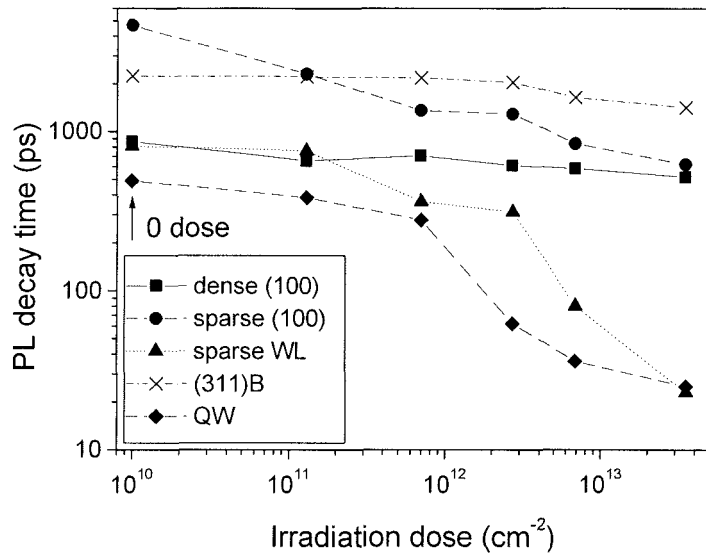


Figure 3. PL decay times for all infrared-emitting QD structures and InGaAs QW for different proton fluences.

irradiation. This may occur due to an additional channel of carrier trapping from the barriers and the WL into the QDs, namely, trapping from the WL to the QDs via radiation-induced defects [7]. Prior to irradiation, carrier transfer from the WL into the dots is inhibited by potential fluctuations in the WL in the low density QDs [8,9]. After irradiation, transfer of these carriers may become possible by trapping to defects and subsequent tunneling into the dots. The similarity of deep-level energies in irradiation-induced defects in GaAs (~0.2 eV) [10] and in the

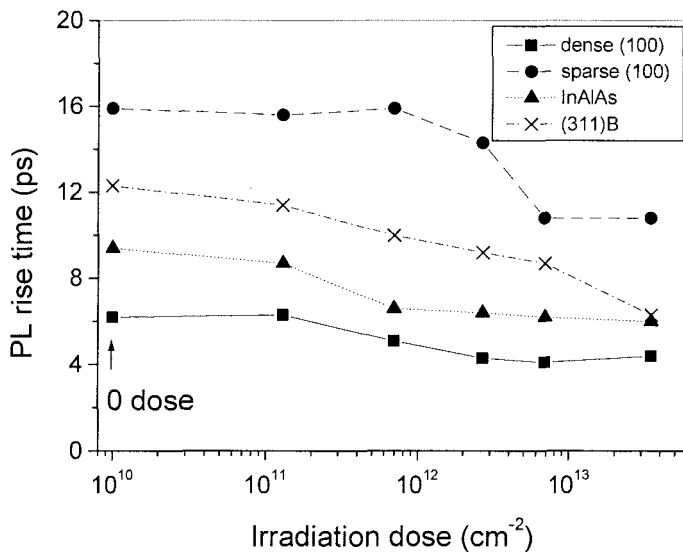


Figure 4. PL rise times for QD structures vs. proton fluence.

small irradiation doses as compared to the un-irradiated QDs.

These observations can be explained if we consider that, unlike in QWs, carriers in the QDs are not mobile and their lifetime is reduced only by the defects created inside the dots. The electrons in the QWs, on the other hand, can easily find radiation-induced traps by moving in the QW plane and be removed from the conduction band.

Enhancement of the PL intensity at low to moderate radiation doses suggests a more effective carrier transfer from the WL into the QDs after

irradiation. This may occur due to an additional channel of carrier trapping from the barriers and the WL into the QDs, namely, trapping from the WL to the QDs via radiation-induced defects [7]. Prior to irradiation, carrier transfer from the WL into the dots is inhibited by potential fluctuations in the WL in the low density QDs [8,9]. After irradiation, transfer of these carriers may become possible by trapping to defects and subsequent tunneling into the dots. The similarity of deep-level energies in irradiation-induced defects in GaAs (~0.2 eV) [10] and in the QDs confining potentials (0.18 – 0.28 eV for different levels) supports this interpretation.

The variations in QD PL rise times are shown as a function of increasing proton dose for all QD samples in Figure 4. QD PL rise times, which reflect carrier capture from the barriers into the dots, decrease with irradiation. This decrease is mainly attributed to the reduction of carrier transport time (due to carrier trapping to defects) in the barriers, from which the carriers are collected into the QDs. The shorter capture times and lower total PL intensities simply reflect the fact that QDs collect only carriers generated closer to the

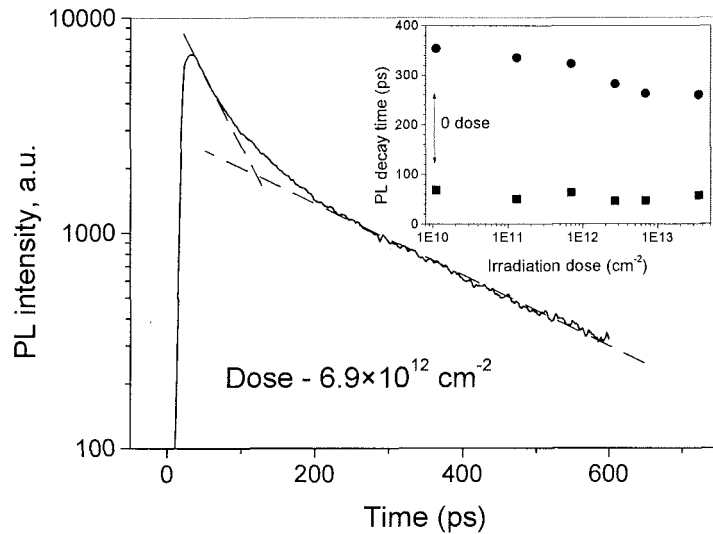


Figure 5. PL transient for InAlAs/AlGaAs QDs with a double-exponential decay. The inset shows the behavior of the long and short decay time components with varying proton dose.

times reported here and by measurements of the temperature dependence of the PL emission, which gave low values ($E_a = 88$ meV) for the activation energy for quenching of the PL emission for these InAlAs dots [11]. This is much lower than the QD confining potentials ($E_{\text{barrier}} - E_{\text{QD}} = 200$ meV). The agreement between activation energies for PL quenching and confining potentials is much better in InGaAs QDs and in MBE grown InAlAs QDs, where there is a lower concentration of growth-related impurities.

The remarkably small decrease in PL peak intensities for InAlAs QDs shown in Figure 2, and the small effect of proton irradiation on their PL decay times shown in Figure 5 demonstrate that when other impurity-related defects are present in QD structures, additional defects introduced by radiation have a very little effect on the PL intensities and QD carrier dynamics, which make these QD structures even more radiation tolerant.

CONCLUSIONS

By means of experimental investigations using time-resolved photoluminescence, we have shown that unlike in QWs, carrier lifetime and dynamics in QDs are not strongly affected by displacement damage defects introduced by 1.5 MeV proton irradiation. This has been proved for irradiation doses up to 3.5×10^{13} cm⁻² on a number of QD structures varying in material, QD surface density and substrate orientation. These findings make QD-based structures attractive candidates for space applications.

ACKNOWLEDGEMENTS

Financial support from the Swedish Foundation for International Cooperation in Research and Higher Education (STINT) and Carl Tryggers Foundation is gratefully acknowledged. Part

dots, since electron-hole pairs excited further away from the QDs can recombine non-radiatively at radiation-induced defect centers

Figure 5 shows PL dynamics for the visibly emitting InAlAs/AlGaAs QDs. Unlike in the other QD samples, the PL decay times can only be fitted with two exponentials. The behavior of the long and short PL decay time components is shown in the inset as a function of proton irradiation. In the unirradiated InAlAs QDs, contrary to InGaAs structures, the carrier lifetimes are governed not by the radiative recombination but by unintentional impurities or defects incorporated into the sample during growth. This interpretation is supported by the shorter PL decay

of this research was carried out at the Jet Propulsion Laboratory, California Institute of Technology, under a contract with the National Aeronautics and Space Administration.

REFERENCES

1. R. Leon, G. M. Swift, B. Magness, W. A. Taylor, Y. S. Tang, K. L. Wang, P. Dowd, and Y. H. Zhang, *Appl. Phys Lett.* **76**, 2074 (2000).
2. P. G. Piva, R. D. Goldberg, I. V. Mitchell, D. Labrie, R. Leon, S. Charbonneau, Z. R. Wasilewski, and S. Fafard, *Appl. Phys Lett.* **77**, 624 (2000).
3. N. A. Sobolev, A. Cavaco, M. C. Carmo, M. Grundmann, F. Heinrichsdorff, and D. Bimberg, *Phys. Stat. Solidi B* **224**, 93 (2001).
4. R. Leon, C. Lobo, J. Zou, T. Romeo, and D. J. H. Cockayne, *Phys. Rev. Lett.* **81**, 2486 (1998).
5. C. Lobo, N. Perret, D. Morris, J. Zou, D. J. H. Cockayne, M. B. Johnston, M. Gal, and R. Leon, *Phys. Rev. B* **62**, 2737 (2000).
6. R. Leon, S. Marcinkevičius, X. Z. Liao, J. Zou, D. J. H. Cockayne, and S. Fafard, *Phys. Rev. B* **60**, R8517 (1999).
7. P. C. Sercel, *Phys. Rev. B* **51**, 14532 (1995).
8. C. Lobo, R. Leon, S. Marcinkevičius, W. Yang, P. C. Sercel, X. Z. Liao, J. Zou, and D. J. H. Cockayne *Phys. Rev. B* **60**, 16647 (1999).
9. S. Marcinkevičius and R. Leon, *Appl. Phys. Lett.* **76**, 2406 (2000).
10. H. A. Jenkinson, G. N. Maracas, M. O'Tooni, and R. G. Sarkis in *Energy Beam-Solid Interactions and Transient Thermal Processing* (Mater. Res. Soc. Proc. Pittsburgh, PA, 1985) pp. p.299-304.
11. C. Lobo, Ph.D. dissertation, Australian National University, March 2000.